VOL 4, NO.1 (2024) 1-15
https://jagst.utm.my

JAGST
Journal of Advanced Geospatial Science & Technology

Application of the Field Hyperspectral Sensing to Estimate the Oxidation-Reduction Potential (ORP) in Tropical Urban Waters

Mohd. Rizaludin Mahmud[1,2*], Soo Kai Ting[1], Nor Wahida Awang[3]
[1]Faculty of Built Environment and Surveying, Universiti Teknologi Malaysia, 81310 Johor Bahru, Johor, Malaysia
[2]Geoscience and Digital Earth Centre, Research Institute for Sustainable Environment (RISE), Universiti Teknologi Malaysia, 81310 Johor Bahru, Johor, Malaysia
[3]Faculty of Applied Sciences, Universiti Teknologi MARA Sarawak, 43000 Kota Samarahan, Sarawak, Malaysia

*Corresponding author: rizaludin@utm.my

Abstract - Oxidation-reduction potential (ORP) is one of the critical water quality parameters used in determining the biochemical condition of water, especially in wastewater treatment. Conventional measurement of ORP requires physical contact with the water samples. A relative version of the ORP measurement that is faster and requires non-contact with the water can be helpful, especially for environmental monitoring. One way to perform this is by measuring the radiated electromagnetic wave from water bodies such as drainage, rivers, and streams that are exposed to sunlight. The reflected radiation from various water samples was obtained using a handheld hyperspectral sensor that is sensitive to 350 – 250 nm radiation and the ORP measurement was performed using the water quality probes sensor equipped with the ORP sensor. Forty-four water samples were taken from multiple locations, including rivers, tributaries, drainage, and streams. Our analysis revealed that the wave spectra at 654 nm can estimate ORP values ranging from 0 to 500 with moderate performance ($R^2 = 0.581$). The reflectance spectra need to undergo normalization, and the second derivative filtering of the Savitsky-Golay is required to obtain such desired results. This preliminary experiment demonstrated that the ORP estimation is plausible using the hyperspectral remote sensor with moderate accuracy for water that potentially experiences nitrification, denitrification, carbonaceous biochemical oxygen demand, and phosphorus waste.

Keywords – *Water biochemical, Savitsky-Golay filter, Water quality*

Article History: Received 14 January 2024, Accepted 25 February 2024, Published 31 March 2024

How to cite: Mahmud, M. R., Ting, S. K. and Awang, N. W. (2024). Application of the Field Hyperspectral Sensing to Estimate the Oxidation-Reduction Potential (ORP) in Tropical Urban Waters. Journal of Advanced Geospatial Science and Technology. 4(1), 1-15.

1.0 Introduction

Oxidation-reduction potential (ORP) or redox is a critical water quality parameter that refers to the measurement of the potential of a water body in oxidizing and reducing another substance. ORP plays a vital role in measuring or determining water quality, especially to indicate possible contamination. ORP helps to describe the respiratory environment of wastewater, whether it is anaerobic, anoxic or aerobic, which are necessary for bacteria to react with nutrient molecules to remove or release certain substances (Ron, 2011; Chen Guang et al., 2017). Knowing ORP in wastewater treatment helps determine the type of biochemical reaction inside the wastewater, thereby promoting or preventing the reaction (Micheal, 2007; Ali & Ali Reza, 2017). The idea is to exploit the spectral changes of the substance of interest, which can be used to identify oxidation-reduction reactions (Yeung et al., 2009).

The current practical and fast method of measuring ORP require physical contact with the water samples using the electronic sensor. However, a fast and non-contact method is necessary for a large area's water quality assessment. The presence of biochemical elements in water can significantly change the properties of the pure water and thus constitute the changes in the reflectance characteristics, particularly in the visible spectrum (Seifi et al., 2019). The hyperspectral remote sensor, which is capable of measuring that reflectance at a narrow bandwidth (~1 nanometer), provides the potential to measure these changes without direct contact with the test solution. Moreover, hyperspectral measurement is one of the most common remote sensing technologies today, and it can function and operate normally even in low light conditions and muddy water (Cunningham & McKee, 2013).

Consequently, hyperspectral reflectance has been widely used to determine and detect water quality based on the water quality parameters' reflectance in many open-water aquatic ecosystems (Sampsa et al., 2002; Rostom et al., 2017). While compared to multispectral remote sensing technology, the main difference of hyperspectral is the hyperspectral has a finer spectral resolution (1nm resolution). Meanwhile, with the development of technology nowadays, field hyperspectral remote sensing, which uses a portable and standalone instrument, a spectroradiometer, has set off a new trend to obtain accurate and detailed spectral information with no constraints on acquisition time from any reachable study site.

Redox reaction produced unique spectral signatures at the molecular level at a specific wavelength. This was demonstrated by Chowdury et al. (2019) for copper, iodine and oxygen molecules; such are significant elements found in environmental water. In that experiment, the effective region of significant absorbance sensitive to copper, iodine and oxygen molecules was identified as somewhere between 420nm, 260nm and 210nm, respectively. Another experiment testing the variant of heme protein myoglobin, which can represent the ability to bind molecular oxygen, was done by Yeung et al. (2009), which indicated the high absorbance of oxidized heme at 400nm and very low absorbance at 500-700nm. Despite this preliminary finding on the potential of hyperspectral sensing to identify chemical reactions, extensive evidence is required to utilize hyperspectral to environmental water samples. This is because the actual condition of environmental water contains varied chemical elements and purity levels.

This study examines whether hyperspectral sensing could estimate the ORP for environmental waters. To materialize this objective, we will investigate the field reflectance spectra from various environmental waters, including rivers, drainage, sewage and channels covering a wide array of suburban and urban landscapes. Effective spectra region will be determined, and its relationship against the actual ORP values will be studied to establish empirical modeling. The output of this experiment would provide helpful information on the potential of field hyperspectral sensors to measure ORP for environmental waters, which can be an alternative tool for a large-scale water quality assessment.

2.0 Materials and Method

2.1 Overall methodology

This study consists of four significant steps: (1) field water sampling, (2) laboratory measurement of the wave spectra and ORP, (3) data processing and modeling, and (4) accuracy assessment. The workflow chart is shown in Figure 1.

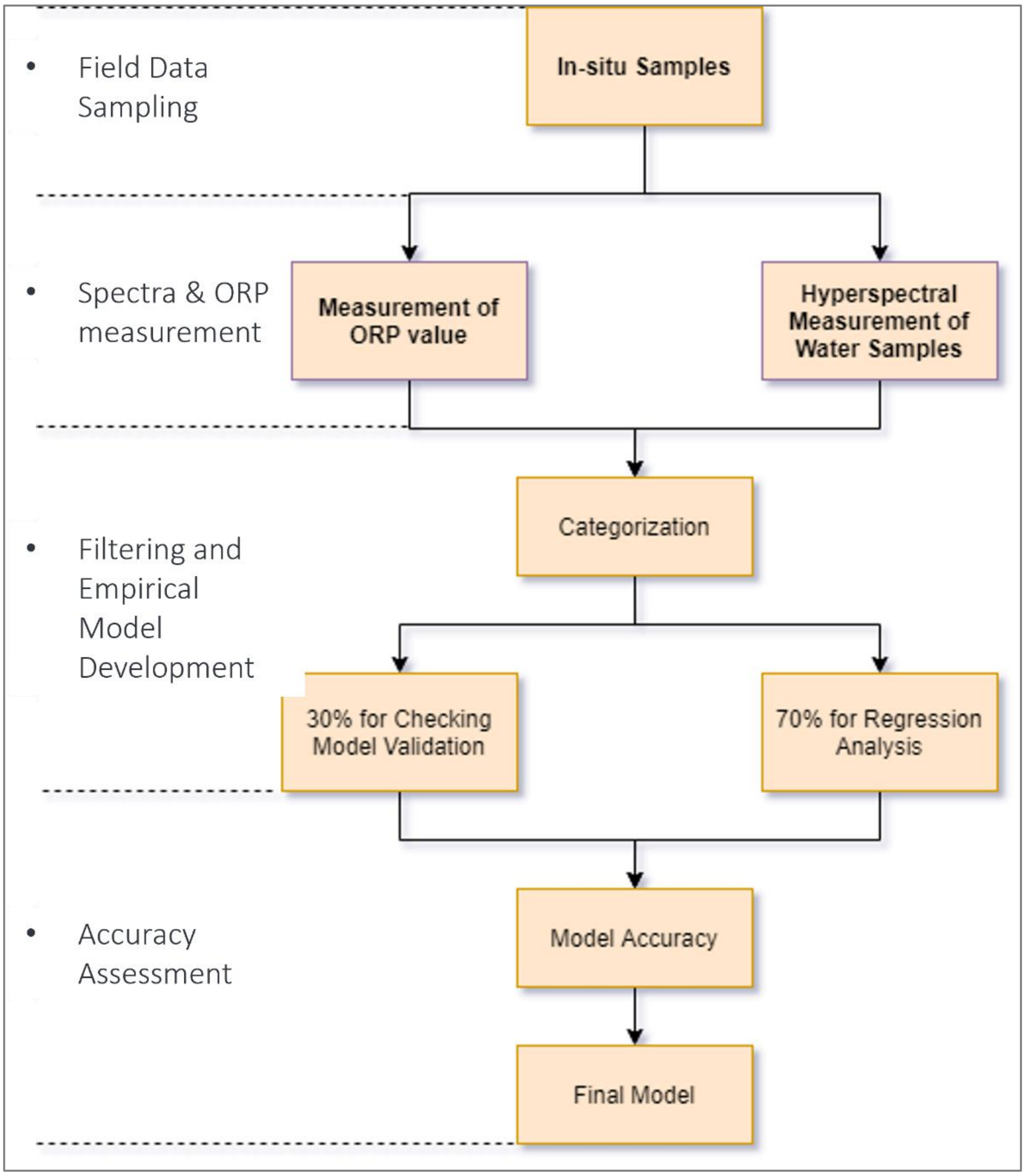

Figure 1. Overall methodology of the study

2.2 Water sampling

Water samples were collected in various Johor river ecosystems, including rivers, tributaries, artificial drainage and natural streams. One litre of samples was obtained using the polyethene bottles. The GPS location of each sampled site was recorded. There are 44 sampling locations, and the selection is based on the various human activities that contributed to a wide range of ORP values, including poultry, agriculture, plantation and aquaculture. Figure 2 illustrates the sampling locations.

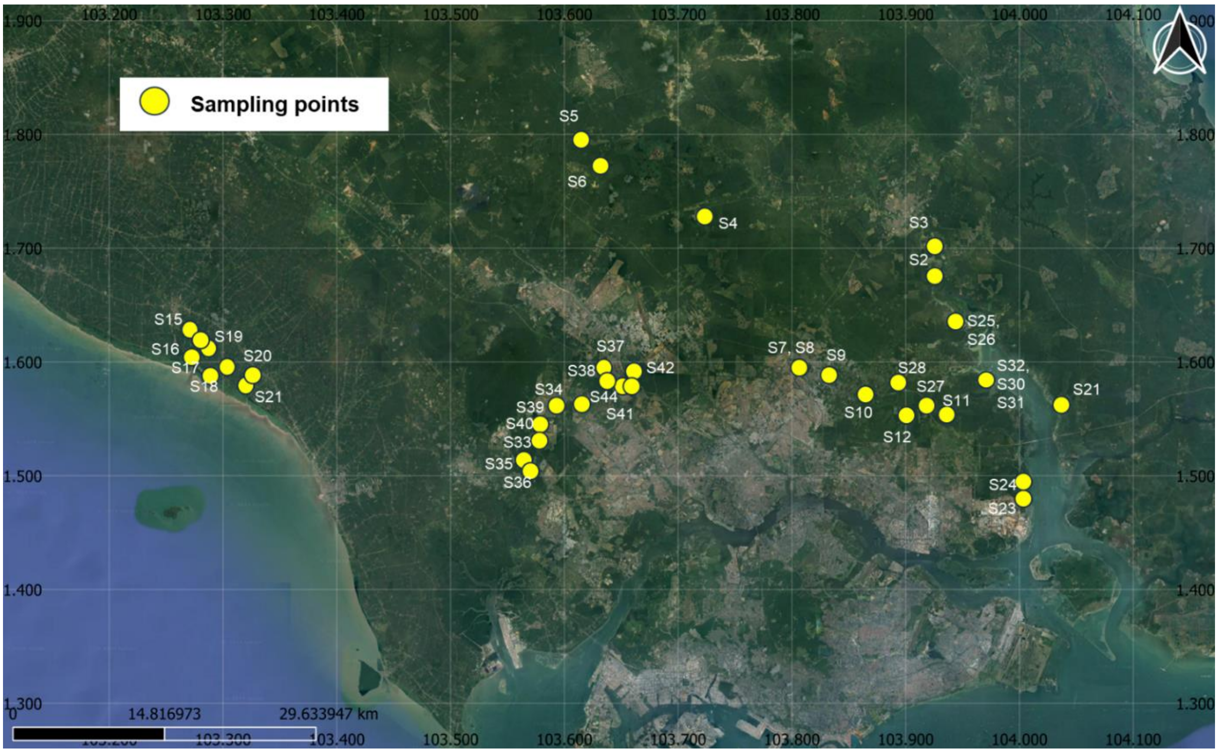

Figure 2. Water sampling locations

2.3 Laboratory measurement

The water samples undergo two laboratory measurements: (1) reflectance spectra and (2) oxidation-reduction potential (ORP). For the reflectance spectra measurement, the Spectral Evolution RS-3500 Spectroradiometer is used. It was a device that used detectors to measure radiation distribution in a specific wavelength region other than photographic film. The specification of the device is shown in Table 1. The scanning geometry of the spectra measurement in the laboratory is described in Figure 3.

Table 1. Specification of Spectral Evolution RS-3500 Spectroradiometer

Specification	Descriptions
Spectral Range	350-2500nm
Spectral Resolution	2.8nm @ 700nm, 8nm @ 1500nm, 6nm @ 2100nm
Spectral Sampling (bandwidth)	Data output in 1nm increments
Minimum Scan Speed	100 milliseconds
Wavelength Accuracy	±0.5 bandwidth
Channels	2151

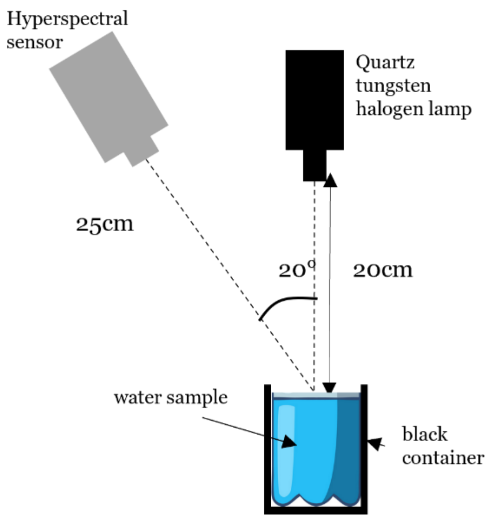

Figure 3. Field spectra measurement schematic diagram

Subsequently, the ORP of the water samples was measured using the Horiba multi-parameter water quality checker version u-50. Table 2 shows the device specifications for a platinum electrode sensitive to the water's electrochemical reaction.

Table 2. Specification of the HORIBA multi-parameter water quality checker

Specification	Descriptions
Measurement Principle	Platinum electrode method
Range	-2000 mV to + 2000mV
Resolution	1 mV
Repeatability	±5 mV
Accuracy	±15 mV

2.4 Data processing and identification of the effective region

The first step in the data processing is data normalization. The minimum and maximum normalization are implemented for the entire spectra. This process is essential to ensure all measurements have a standard normalized baseline (Julian et al., 2019). After normalization, a Savitzky-Golay second spectral derivative with 21 smoothing points and 2nd order polynomial were computed (Mancini, et al., 2019). Savitzky-Golay derivative was used as it can be a good noise filter by removing the background due to scattering (Indrajit , 2019). The derivatives of spectra help to reveal information in a spectrum. First, a polynomial regression was performed on the normalized spectra on the data points in the moving window, followed by the first and second-order derivatives. The formula of polynomial regression used is given:

$$F(x) = a_n x^n + a_{n-1} x^{n-1} + a_{n-2} x^{n-2} + \ldots + a_1 x + a_0 \quad (3.1)$$

Meanwhile, the expression of the first derivative used is given as

$$F'(x) = n a_n x^{n-1} + (n-1)\, a_{n-1} x^{n-2} + \ldots + a_1 \quad (3.2)$$

Besides that, the algorithm of the second derivative used is

$$F''(x) = n(n-1)\, a_n x^{n-2} + (n-2)(n-1)\, a_{n-1} x^{n-3} + \ldots \quad (3.3)$$

Where n is polynomial order and ai, i=0,…n is fitted coefficients.

Consequently, the normalized and filtered reflectance spectra will be regressed against the ORP. The reflectance spectra at specific regions with the highest correlation would be identified and extracted from the regression model. Only 70% of the samples were used in the modeling process, while 30% were used for accuracy evaluation. The ORP values between the modelled and actual ORP were compared to validate the regression model. If the value fell between a similar range of biochemical reactions (Table 3), it was considered valid and vice versa.

Table 3. ORP value and potential biochemical reaction. (Source: Gerard, H. 2015)

Biochemical reaction	**ORP, mV**
Reduction of nitrate	+300 to +600
Reduction of manganese	+220 to +500
Reduction of iron	+180 to +400
Nitrification	+100 to +350
Reduction of sulfate	+100 to -200
COD degradation	+50 to +250
Biological phosphorus removal	+25 to +250
Denitrification	+50 to -50
Sulfide formation	-50 to -250
Acid formation	-100 to -225
Biological phosphorus release	-100 to -250
Methane production	-175 to -400

3.0 Result and Discussion

3.1 Field sample ORP values

Based on Figure 4 and the guidelines of Table 3, it showed that the ORP values for every sampling station had positive values. Most of the water potentially had ORP values from 100 to 200, indicating that nitrification, COD degradation, and biological phosphorus removal reactions dominate. Meanwhile, a significant number of stations had higher ORP values from 250 – 480. Such biochemical plausible responses could include reduced nitrate, manganese, iron, and nitrification. A few samples had negative ORP values and potentially experienced a reduction in the sulfate reaction. In summary, the samples taken provide slightly biased measurements towards positive ORP.

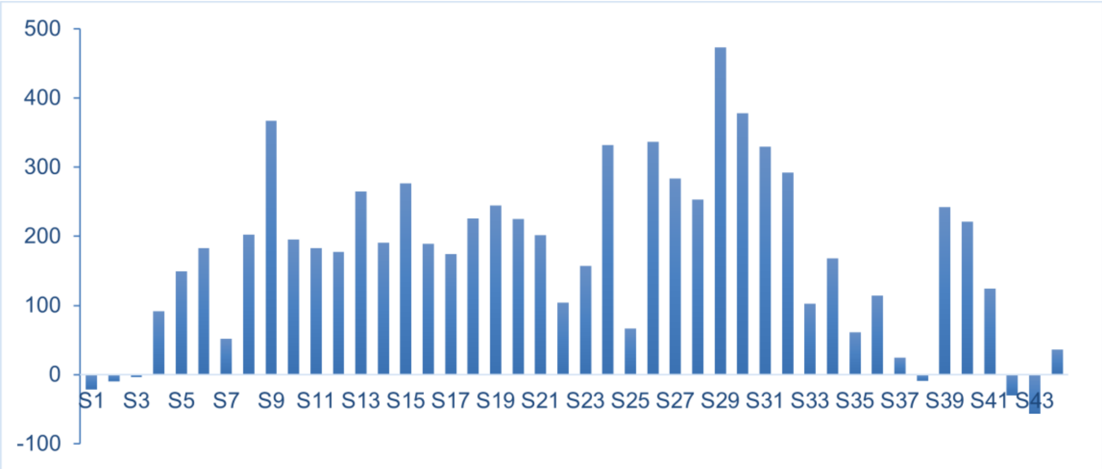

Figure 4. ORP value of the field samples

3.2 Processed reflectance spectra

Figure 5 shows the pre-processed reflectance spectra that have undergone normalization. Normalization helps to transform the reflectance spectra into one standard reference reflectance (Figure 5b). Six potential spectra regions were identified upon the normalization process as they showed significantly high differences in reflectance pattern among the samples (Figure 6a). Table 4 shows all the respective regions.

However, the first region seems more promising due to the following reasons; first the separation line is greater and the gradual linear reflectance increment indicates possibilities of linear relationship with ORP. Secondly, the rest of the region, 2 – 6, has more significant noise (not a smooth line). Consequently, the first region's spectra were selected to undergo Savitsky-Golay filtering to reduce the noise and increase the sensitivity of the separation. Figure 6b shows the filtered spectra and the centre of the wavelength range.

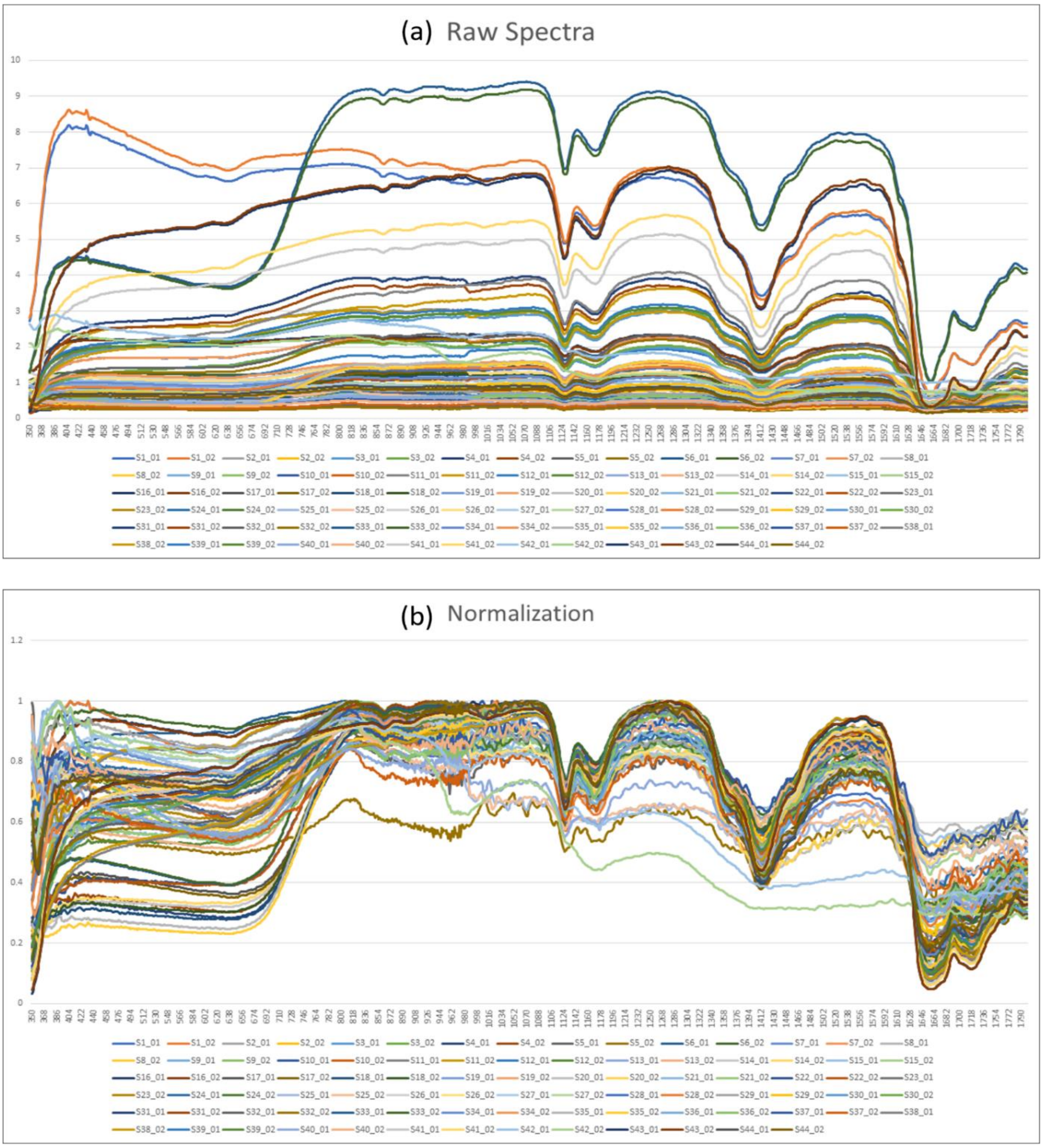

Figure 5. Hyperspectral reflectance from water samples. (a) Raw spectra and (b) Normalized and filtered spectra

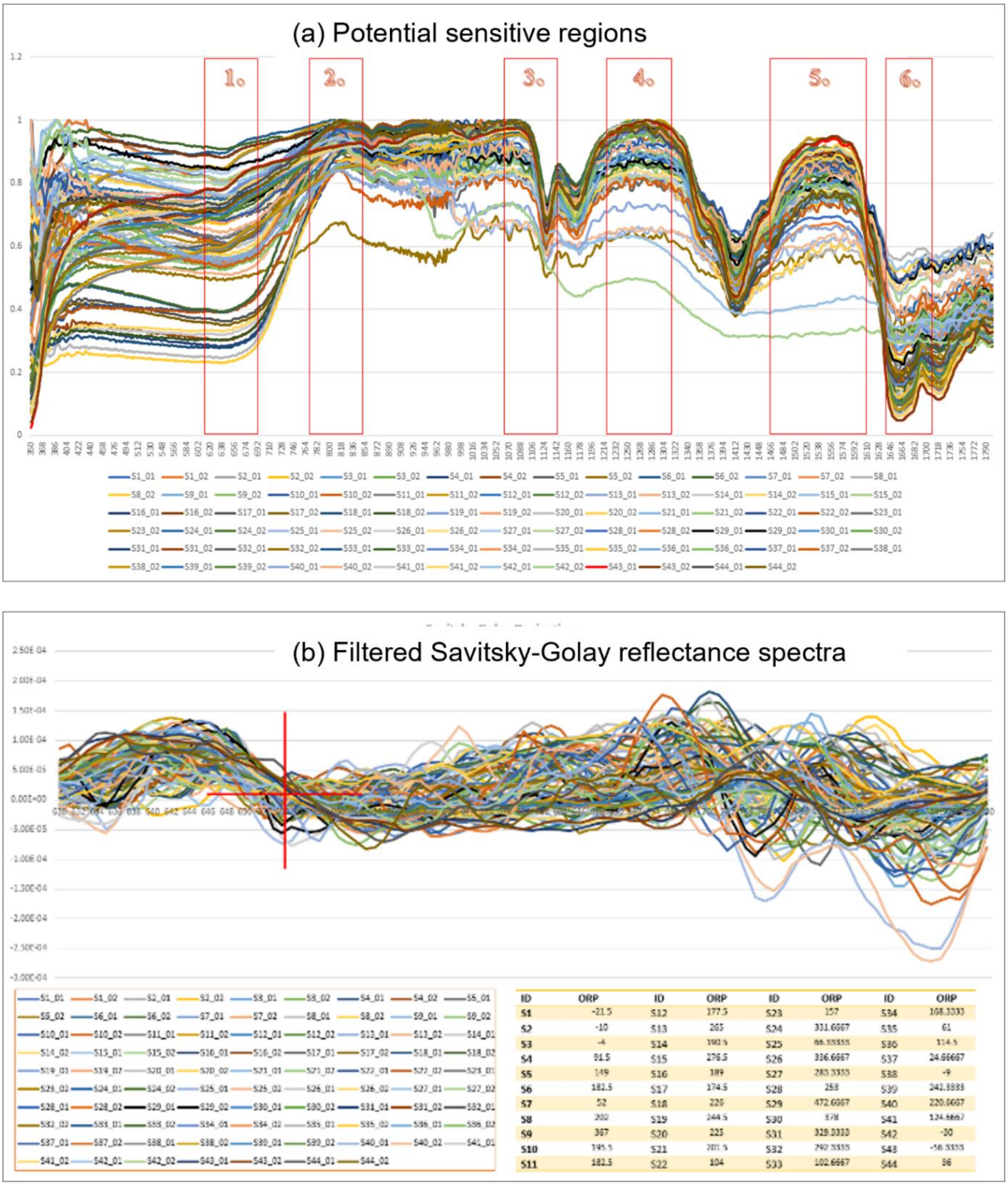

ID	ORP	ID	ORP	ID	ORP	ID	ORP
S1	-21.5	S12	177.5	S23	157	S34	168.3333
S2	-10	S13	265	S24	331.6667	S35	61
S3	-4	S14	193.5	S25	86.33333	S36	114.5
S4	91.5	S15	276.5	S26	336.6667	S37	24.66667
S5	149	S16	189	S27	283.3333	S38	-9
S6	182.5	S17	174.5	S28	253	S39	241.3333
S7	52	S18	226	S29	472.6667	S40	220.6667
S8	202	S19	244.5	S30	378	S41	124.6667
S9	367	S20	225	S31	329.3333	S42	-30
S10	195.5	S21	201.5	S32	292.3333	S43	-56.3333
S11	182.5	S22	104	S33	102.6667	S44	36

Figure 6. Processed filtered spectra. (a) Potential sensitive region and (b) Filtered Savitsky – Golay reflectance spectra

Table 4. Sensitive region and its respective wavelength range

Region	Wavelength
1	620nm – 720nm
2	770nm – 820nm
3	1070nm – 1150nm
4	1210nm – 1330nm
5	1460nm – 1610nm
6	1640nm – 1700 nm

3.3 ORP sensitive region, regression model and accuracy assessment

Results from the Savitsky-Golay filter identified that the region of wavelength in 654 had the highest linear trend and decent correlation with the ORP. The coefficient of determination value score was 58%, indicating the model could have fair strength (Figure 7). The model, however, was limited to -50 ORP values, which made it unable to represent the solid biochemical reaction of sulfide formation, biological phosphorus release, acid formation, and methane production.

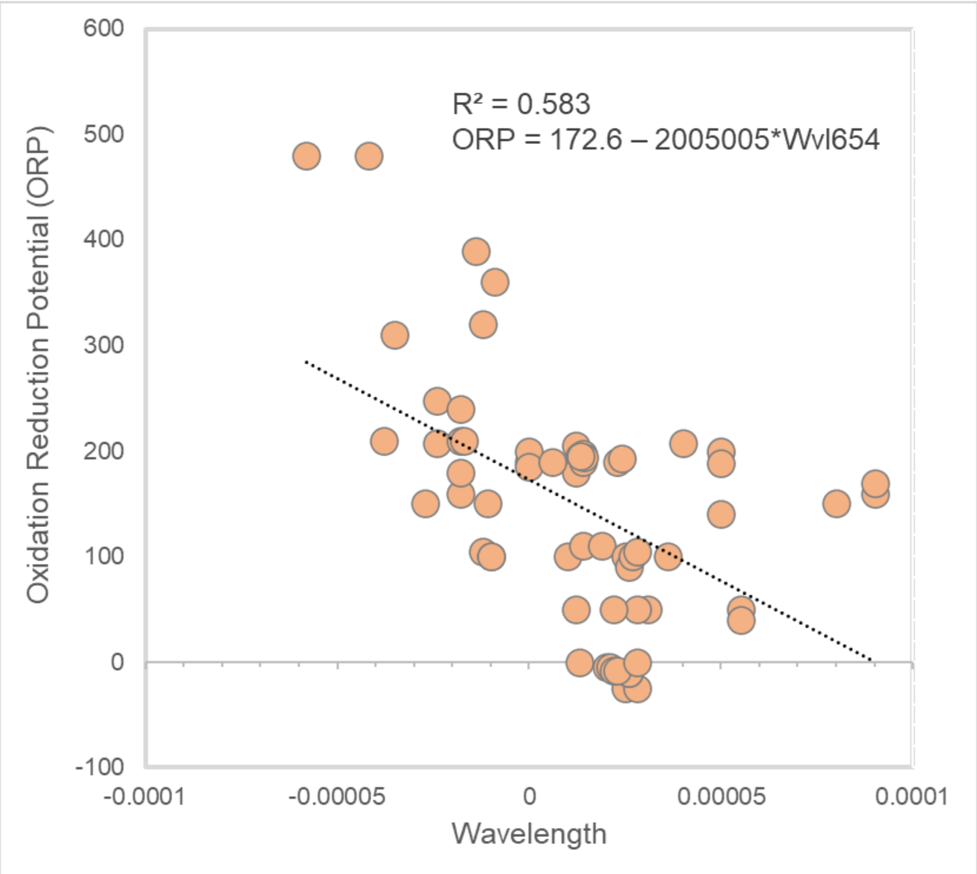

Figure 7. ORP scatter plot and regression model

Validation against the independent dataset showed moderate performance with 54% agreement (Table 5). Nevertheless, considering it was based on boolean logic evaluation (true or false), most of the modelled ORP value was within the actual condition range. This showed that the model could represent the actual ORP value by sensing the spectral reflectance at 654nm. Although the accuracy is just fair, this preliminary experiment showed that there was a potential to utilize spectral reflectance measurement for rapid ORP assessment.

Table 5. Accuracy assessment

ID	Biochemical Reaction & ORP Value				Remarks
	Observed		Modelled		
S13_01	Nit, Biophop	265	Nit, Biophop, cBOD	220	TRUE
S13_02	Nit, Biophop	265	Biophop, Deni	50	FALSE
S15_01	Nit.	277	Biophop, cBOD	160	FALSE
S15_02	Nit.	277	Nit, Biophop, cBOD	248	TRUE
S21_01	Nit, cBOD	202	Nit, Biophop, cBOD	200	TRUE
S21_02	Nit, cBOD	202	Nit, Biophop, cBOD	198	TRUE
S25_01	Nit, Biophop, cBOD	66	Nit	110	TRUE
S25_02	Nit, Biophop, cBOD	66	Nit, Biophop, cBOD	110	TRUE
S26_01	Nit.	337	Nit	300	TRUE
S26_02	Nit.	337	Nit, Biophop, cBOD	300	TRUE
S27_01	Nit.	283	Nit, Biophop, cBOD	220	TRUE
S27_02	Nit.	283	Nit, Biophop, cBOD	220	TRUE
S28_01	Nit.	253	Nit, Biophop, cBOD	190	TRUE
S28_02	Nit.	253	Nit, Biophop, cBOD	191	TRUE
S30_01	Nit.	378	Biophop, cBOD	230	FALSE
S30_02	Nit.	378	Nit, Biophop, cBOD	248	TRUE
S31_01	Nit, Biophop	329	Nit, Biophop, cBOD	290	TRUE
S31_02	Nit, Biophop	329	Biophop, cBOD	220	FALSE
S32_01	Nit, Biophop	292	Biophop, cBOD	220	FALSE
S32_02	Nit, Biophop	292	Biophop, cBOD	220	FALSE
S37_01	Biophop,Deni	25	Nit, Biophop, cBOD	85	FALSE
S37_02	Biophop,Deni	25	Biophop, cBOD	85	FALSE
S38_01	Deni	-9	Nit, Biophop, cBOD	120	FALSE
S38_02	Deni	-9	Nit, Biophop, cBOD	120	FALSE
S39_01	Nit, Biophop, cBOD	242	Biophop, cBOD	162	FALSE
S39_02	Nit, Biophop, cBOD	242	Nit, Biophop, cBOD	200	TRUE
			TRUE		14
			FALSE		12
			Average accuracy		53.85%

4.0 Discussion

The derived hyperspectral-ORP model had limited representation from -50 and below. This indicates that the hyperspectral-ORP model had limited sensitivity to the water that experienced a colourless biochemical reaction or one that did not cause significant changes to the water turbidity. This is because all the biochemical reactions of sulfide formation, biological phosphorus release, acid formation, and methane production resulted in a colourless impact on the water (Verma and Ratan, 2020; Hassan Omer, 2020; Fu et al., 2023). In addition, corresponding results shown by Avdan et al. (2019) and Mohamed (2019) also revealed that a significant relationship between satellite reflectance and turbid waters was indicated in the red region (600-660nm). This signified that the hyperspectral-ORP model could be influenced by the light attenuation by the presence of larger pollutants resulting from removing the chemical from significant physical elements like soil, especially in agriculture and urban drainage disposal.

Nonetheless, despite the fair strength of the hyperspectral ORP model as well as its performance, it can be compensated by the advantages of its fast, non-destructive and non-contact approach. It can be helpful in a few circumstances. The first is when the field sampling is complex or restrained, such as in confidential or private areas, fast-flowing rivers or drainage, heavily polluted waters, or river ecosystems with dangerous wildlife habitats. Secondly, if the hyperspectral sensing is done using an unmanned aerial vehicle (UAV) or drone, it also could provide a rapid preliminary assessment of the water redox potential. This is particularly useful during tragic water pollution incidents such as massive waste dumping oil or slurry spills (e.g., Rahman, 2011; The Malay Mail, 2023).

5.0 Conclusion

This experiment demonstrated the potential of determining the oxidation-reduction potential in environmental water samples using the field hyperspectral measurement. The result showed that appropriate normalization and Savitsky-Golay filtering enabled better representation of spectral reflectance relationship with ORP values at 654nm wavelength. The obtained regression model has fair representation ($r^2 = 0.58$) and fair Boolean accuracy of 54%. The proposed method offers a quick but rough estimate of the biochemical reaction redox, ORP, with moderate accuracy and a non-contact approach.

Acknowledgement

This research was part of the Research Funding Initiatives on the following project, Projecting the Near Future of Worst Micro-Climate Scenarios in Urbanized Tropics City using Big-Geospatial Data (Q.J130000.2652.17J09) and Fundamental Research Grant Scheme by Ministry of Higher Education Malaysia (R.J130000.7852.5F378) and the UTM ICONIX Research Project on Sustainable Tropical Coastal Communities (Q.J130000.4352.09G76).

Conflict of Interest

The authors declare no conflict of interest.

References

Ali, R. S., Alireza, P. (2017). The application of oxidation reduction potential (ORP) sensor in water and wastewater treatment industries. Journal of Env. Res. Tech. Vol. 1, 15 - 21.

Avdan, Z. Y., Kaplan, G., Göncü, S., & Avdan, U. (2019). Monitoring the water quality of small water bodies using high-resolution remote sensing data. ISPRS International Journal of Geo-Information, 8(12), 553. https://doi.org/10.3390/ijgi8120553

Chen-Guang Liu, Jin-Cheng Qin, Yen-Han Lin (2017). Fermentation and Redox Potential, Fermentation Processes, Angela Faustino Jozala, IntechOpen, DOI: 10.5772/64640.

Chowdhury, B., Mondal, M. H., Barman, M. K., & Saha, B. (2019). A study on the synthesis of alkaline copper(III)-periodate (DPC) complex with an overview of its redox behavior in aqueous micellar media. Research on Chemical Intermediates, 45(2), 789-800.

Fu, L., You, S., Li, G. Zengchang, F. (2023). Enhancing methane sensing with NDIR technology: Current trends and future prospects, Reviews in Analytical Chemistry, vol. 42, no. 1, 2023, pp. 20230062. https://doi.org/10.1515/revac-2023-0062.

Hassan Omer, N. (2020). Water Quality Parameters. IntechOpen. doi: 10.5772/intechopen.89657.

Indrajit , G. (2019). An optimal Savitzky–Golay derivative filter with geophysical.

Julian, G., Anne, G.-B., & Bruno, B. (2019). Critical review and advices on spectral-based normalization methods for LIBS quantitative analysis. Spectrochimica Acta Part B: Atomic Spectroscopy, 160, 105688.

Mancini, M., Rinnan, Å., Pizzia, A., & Toscano, G. (2019). Use of Fourier transform near infrared spectroscopy for the detection of residues from wood processing industry in the pellet sector. Proc. 18 77 th Int. Conf. Near Infrared Spectrosc.

Micheal, H. (2007). ORP Management in Wastewater as An Indicator of Process Efficiency. NEIWPCC’s newsletter, Interstate Water Report.

Mohamed, G. A. I. (2019). Shallow water empirical remote sensing bathymetry using the blue/green and red spectrum regions. Journal of Scientific Research and Reports, 1-8. https://doi.org/10.9734/jsrr/2019/v22i330091.

Rahman, H. A. (2021). Water Issues in Malaysia. International Journal of Academic Research in Business and Social Sciences, 11(8), 860-875.

Ron, T. (2011). It’s Not Black Magic. Retrieved from TPO-Treatment Plant Operator: https://www.tpomag.com/editorial/2011/10/its_not_black_magic

Rostom, N. G., Shalaby, A. A., Issa, Y. M., Afifi, A. A. (2017). Evaluation of Mariut Lake water quality using hyperspectral remote sensing and laboratory works. The Egyptian Journal of Remote Sensing and Space Science. Vol. 20, 1, 39 – 48.

Sampsa, K., Jouni, P., Kari, K., & Martti, H. (2002). Lake water quality classification with airborne hyperspectral spectrometer and simulated MERIS data. Remote Sensing of Environment (79), 51-59.

Seifi, A., Hossein, M., Ranjbar, H., Honarmand, M. (2019). Visible-infrared spectroscopy and chemical properties of water in mining area. Water Sci Technol. 80, 9, 1612 – 1622.

The Malay Mail (2023). Air Selangor: Four water treatment plants resume operations after odour pollution incident. The Malay Mail. https://www.malaymail.com/news/malaysia/2023/02/12/air-selangor-four-water-treatment-plants-resume-operationsafter-odour-pollution-incident/54564.

Verma, P., Ratan, J. K. (2020). Assessment of the negative effects of various inorganic water pollutants on the biosphere—an overview, Editor(s): Pooja Devi, Pardeep Singh, Sushil Kumar Kansal, Inorganic Pollutants in Water, Elsevier, 73-96.

Yeung, N., Lin, Y.-W., Gao, Y.-G., Zhao, X., Russell, B., Lei, L., Lu, Y. (2009). Rational design of a structural and functional nitric oxide reductase. Nature.